

# Triple-Band SiGe HBT Clapp and Hartley Oscillators Using Stacked Element-Selective Transistors

Hikaru Ikeda and Yasushi Itoh

Shonan Institute of Technology  
1-1-25 Tsujido-Nishikaigan, Fujisawa, Kanagawa, 251-8511 Japan

This article is distributed under the Creative Commons by-nc-nd Attribution License.  
Copyright © 2019 Hikari Ltd.

## Abstract

This paper presents triple-band SiGe HBT Clapp and Hartley oscillators for the next generation multi-band and multi-mode wireless radios. The oscillators connect a stacked element-selective transistor in parallel with two circuit elements and can provide a triple-band oscillation by switching only two circuit elements. The stacked element-selective transistor is a two-terminal device with base and collector short-circuited and thus can provide three different conditions of open, short and small capacitance. A triple-band oscillation becomes available by using these conditions. The implemented 0.35  $\mu\text{m}$  SiGe HBT Clapp VCO has achieved a low-band oscillation of 0.81 GHz, a middle-band oscillation of 0.92 GHz, and a high-band oscillation of 1.01 GHz. The phase noise at 100 kHz offset varies from -93 to -102 dBc/Hz. On the other hand, the implemented 0.35  $\mu\text{m}$  SiGe HBT Hartley VCO has achieved a low-band oscillation of 0.98 GHz, a middle-band oscillation of 1.04 GHz, and a high-band oscillation of 1.22 GHz. The phase noise at 100 kHz offset varies from -84 to -94 dBc/Hz.

**Keywords:** microwaves, multi-band, Clapp oscillator, Hartley oscillator, stacked element-selective transistor, SiGe HBT

## 1 Introduction

Multi-band and multi-mode VCOs have gathered much attention in the next generation multi-band and / or multi-mode wireless radios for a miniaturized size

of the circuit and module [1], [8]. Up to now, a variety of multi-band VCOs had been reported: a traveling wave VCO [2], an active inductor VCO [9], a transformer-coupled VCO [7] and a triple-band frequency generator using QVCO and Gilbert cell mixers [10]. Indeed, these VCOs can provide excellent multi-band performances, but require a number of circuit elements. Therefore, the circuit becomes much complicated in configuration, large in size and lossy in performance. In order to address these problems, the authors have presented novel switching techniques and multi-band resonators: a supply voltage switching [4], a forward / backward-bias switching [3], and a reconfigurable multi-band resonator [5]. As an alternative design approach, the authors have also shown a triple-band cross-coupled differential VCO with stacked element-selective transistors [6]. It has provided a triple-band oscillation by switching only two circuit elements. In this paper, the design, simulation, fabrication and, performance of the triple-band Clapp and Hartley oscillators using the stacked element-selective transistors are presented.

## 2 Circuit Design and Simulation

A schematic diagram of the triple-band Clapp and Hartley oscillators using the stacked element-selective transistors is shown in Fig. 1. The oscillators employ a common-collector configuration and thus an output signal can be derived from the emitter.  $Q_1$  is a common-collector transistor and  $R_E$  is an emitter resistor for controlling a total current.  $L_C$  is a shunt coil for controlling a negative impedance generation.  $R_{B1}$  and  $R_{B2}$  is a base bias resistor.  $C_C$  is a decoupling capacitor. The oscillators employ a triple-band resonator comprised of a parallel LC circuit ( $L_1$ ,  $L_2$ ,  $C_1$ ,  $C_2$ , and  $C_3$ ) and stacked element-selective transistors ( $Q_2$ ,  $Q_3$ ). The stacked element-selective transistors are a two-terminal device with base and collector short-circuited and thus can provide three different conditions of open, short and small capacitance. A triple-band oscillation becomes available by using these conditions.  $V_C$  is a control voltage. A triple-band resonance can be obtained by setting a control voltage of  $V_C$  to  $-1V$ ,  $0V$  or  $+1V$ .

A schematic diagram of the triple-band Clapp and Hartley resonators using the stacked element-selective transistors is demonstrated in Fig. 2. The stacked element-selective transistors provide three different resonators. For  $V_C = -1V$ ,  $Q_3$  is short and  $Q_2$  is open. That is, only  $L_1$  is selected in Clapp-type and only  $C_1$  is selected in Hartley-type. On the other hand, for  $V_C = +1V$ ,  $Q_2$  is short and  $Q_3$  is open. That is, only  $L_2$  is selected in Clapp-type and only  $C_2$  is selected in Hartley-type. For  $V_C = 0V$ , both  $Q_2$  and  $Q_3$  become small capacitance. That is, both  $L_1$  and  $L_2$  are selected in Clapp-type and both  $C_1$  and  $C_2$  are selected in Hartley-type. A low-band resonant frequency ( $f_L$ ), a middle-band resonant frequency ( $f_M$ ) and a high-band resonant frequency ( $f_H$ ) can be given as follows:

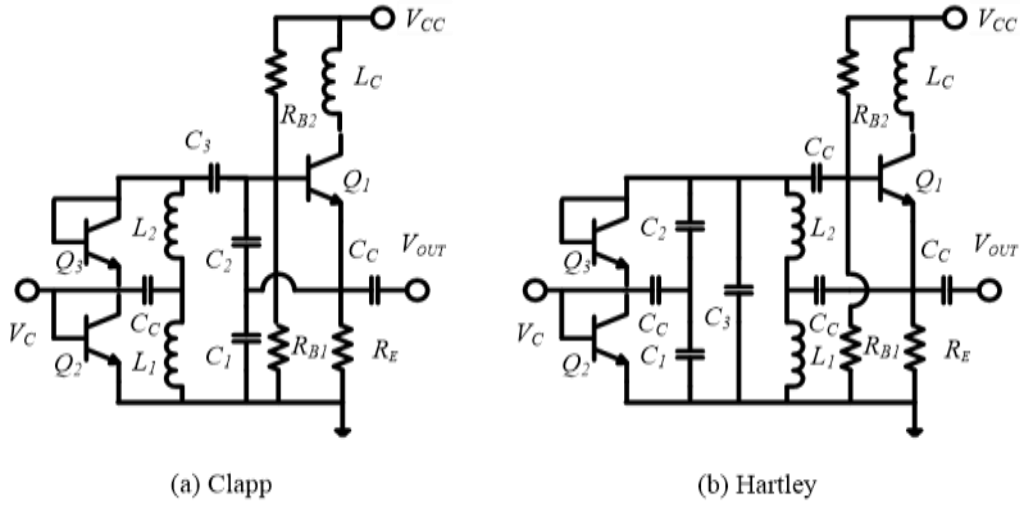


Fig. 1 Schematic diagram of the triple-band Clapp and Hartley oscillators using the stacked element-selective transistors.

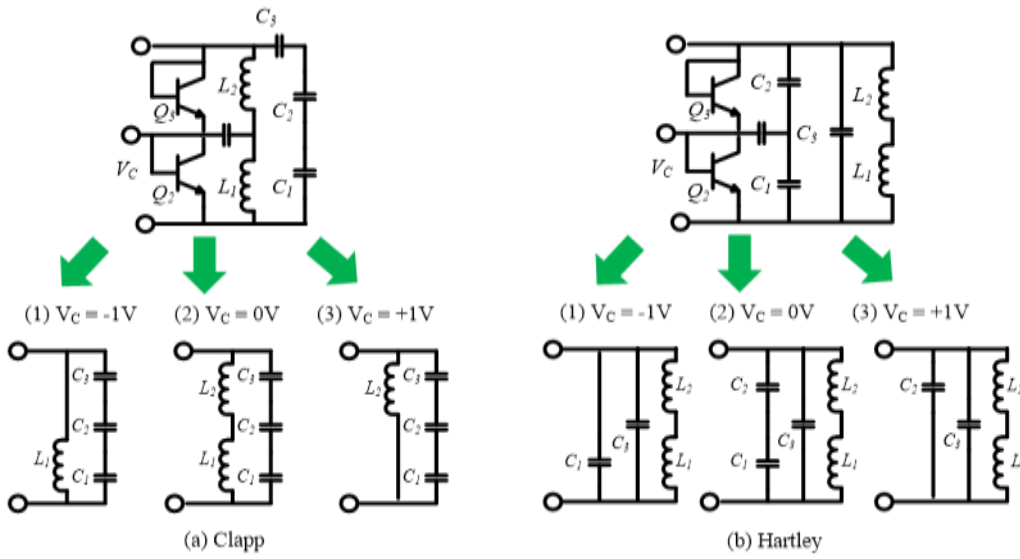


Fig. 2 Schematic diagram of the triple-band Clapp and Hartley resonators using the stacked element-selective transistors.

< Clapp-type >

$$f_L = \frac{1}{2\pi} \sqrt{\frac{1/C_1 + 1/C_2 + 1/C_3}{L_1 + L_2}} \quad (1)$$

$$f_M = \frac{1}{2\pi} \sqrt{\frac{1/C_1 + 1/C_2 + 1/C_3}{L_2}} \quad (2)$$

$$f_H = \frac{1}{2\pi} \sqrt{\frac{1/C_1 + 1/C_2 + 1/C_3}{L_1}} \quad (3)$$

< Hartley-type >

$$f_L = \frac{1}{2\pi \sqrt{(L_1 + L_2)(C_2 + C_3)}} \quad (4)$$

$$f_M = \frac{1}{2\pi \sqrt{(L_1 + L_2)(C_1 + C_3)}} \quad (5)$$

$$f_H = \frac{1}{2\pi} \sqrt{\frac{C_1 + C_2}{(L_1 + L_2)(C_1 C_2 + C_2 C_3 + C_3 C_1)}} \quad (6)$$

It is assumed in Equations (1) to (6) that  $L_1$  is smaller than  $L_2$  for Clapp-type and that  $C_1$  is smaller than  $C_2$  for Hartley-type. The circuit element values consisting of the triple-band resonator are summarized in Table 1 for Clapp-type and Table 2 for Hartley-type, respectively.  $f_L$ ,  $f_M$  and  $f_H$  are calculated by using Equations (1) to (6) as well as Tables 1 and 2. The calculated results are plotted in Fig. 3 for Clapp-type and Fig. 4 for Hartley-type. It is clearly demonstrated that a triple-band resonance has been obtained by switching a control voltage of  $V_C$ .

Table 1 Circuit element values of Clapp-type.

Element	Value	Element	Value
$C_1$ [pF]	6	$C_C$ [pF]	1000
$C_2$ [pF]	7	$L_1$ [nH]	5.1
$C_3$ [pF]	3	$L_2$ [nH]	7.5

Table 2 Circuit element values of Hartley-type.

Element	Value	Element	Value
$C_1$ [pF]	1.5	$L_1$ [nH]	1
$C_2$ [pF]	3	$L_2$ [nH]	1
$C_C$ [pF]	1000		

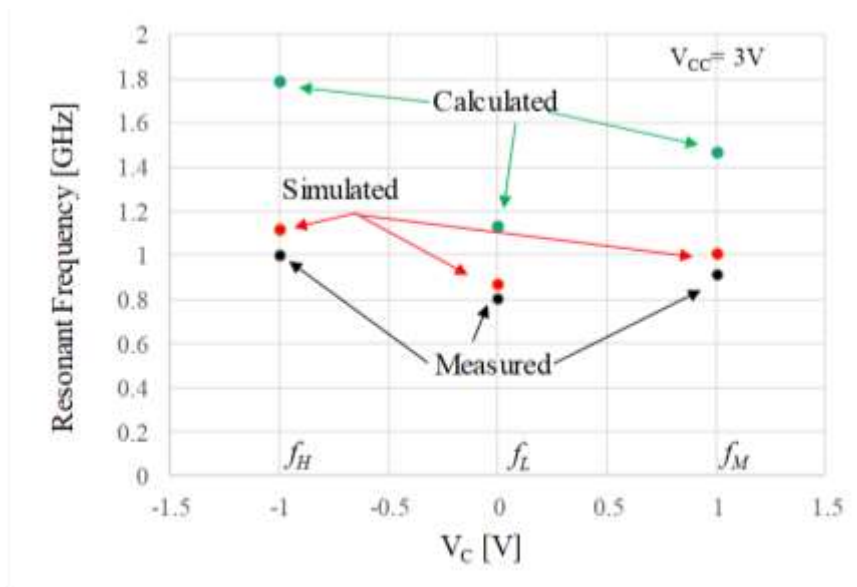


Fig. 3 Calculated, simulated and measured resonant frequencies of Clapp-type.

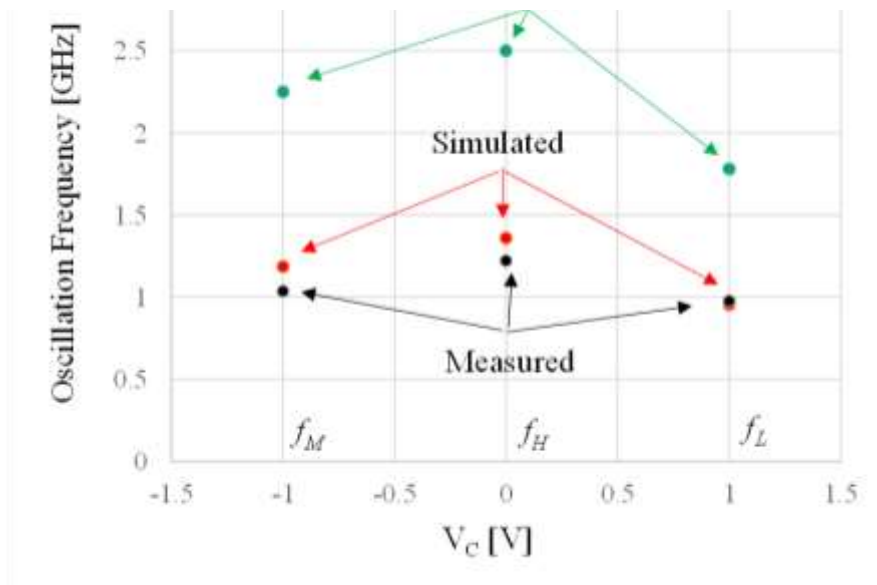
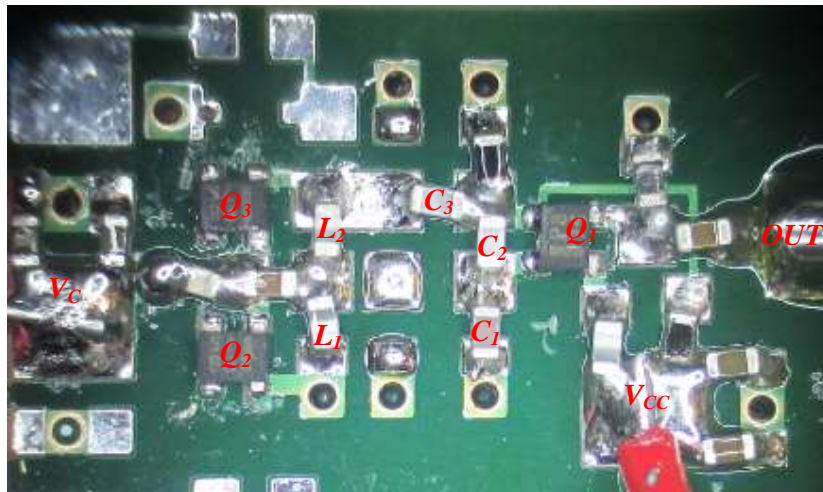


Fig. 4 Calculated, simulated and measured resonant frequencies of Hartley-type.

The circuit simulation has been accomplished for the schematic diagram of Fig. 1 by using ADS of Keysight Technologies. The simulated oscillation frequencies are also plotted in Figs. 3 and 4. The simulated oscillation frequencies become lower than the calculated resonant frequencies. It is because the intrinsic and parasitic elements of chip and distributed devices are actually included in the simulation. The precise nonlinear transistor model is also taken into account in the simulation. In the simulation, a supply voltage of  $V_{CC}$  was determined as 3V.

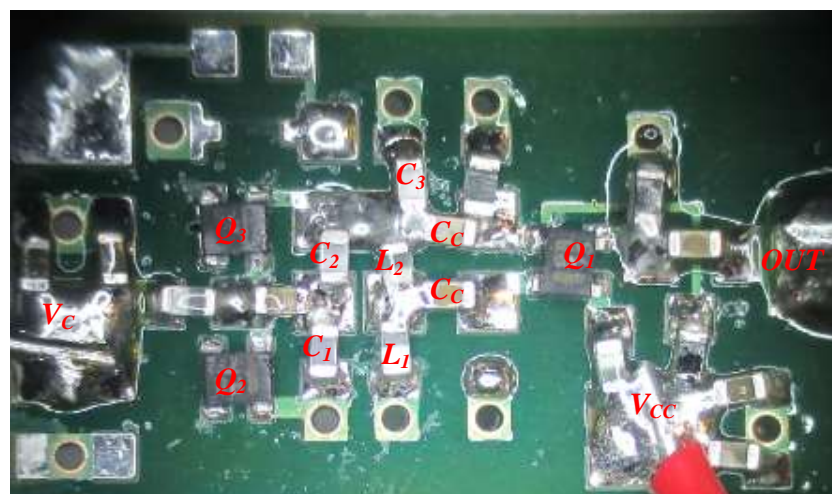
### 3 Circuit Fabrication and Performance

Photographs of the triple-band Clapp and Hartley oscillators using the stacked element-selective transistors are depicted in Figs. 5 and 6, respectively. The oscillators were fabricated on the FR-4 substrate with a dielectric constant of  $4.4@1\text{GHz}$  and a  $\tan\delta$  of  $0.016@1\text{GHz}$ . 1005-type chip resistors, capacitors, and inductors are mounted on the substrate by soldering. A surface mount type of the  $0.35\mu\text{m}$  SiGe HBT with an  $f_t$  of around 25 GHz (Toshiba MT4S102T) is used as an oscillator device as well as a switching device. The circuit size is  $8 \times 14 \times 1.2 \text{ mm}^3$ , respectively.



$8 \times 14 \times 1.2 \text{ mm}^3$

Fig. 5 Photograph of the triple-band Clapp oscillator.



$8 \times 14 \times 1.2 \text{ mm}^3$

Fig. 6 Photograph of the triple-band Hartley oscillator.

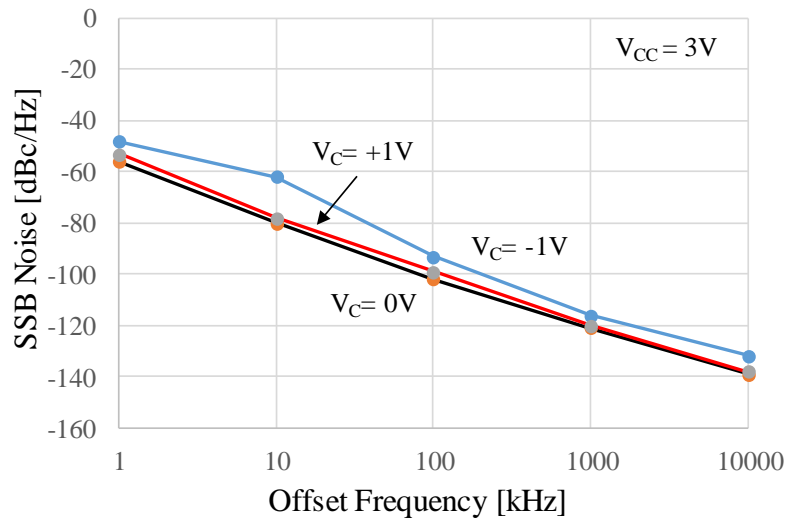


Fig. 7 Measured SSB noise of the triple-band Clapp oscillator.

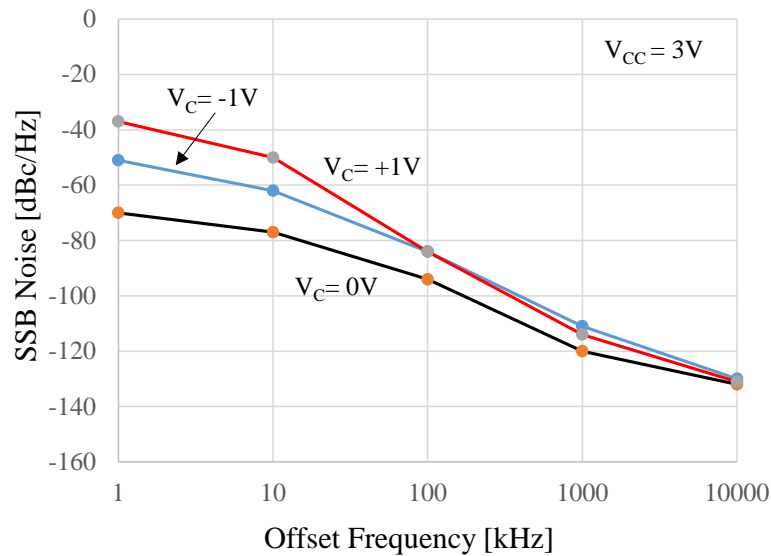


Fig. 8 Measured SSB noise of the triple-band Hartley oscillator.

Measured oscillation frequencies are also shown in Figs. 3 and 4, respectively. The triple-band Clapp VCO has achieved a low-band oscillation of 0.81 GHz, a middle-band oscillation of 0.92 GHz, and a high-band oscillation of 1.01 GHz. On the other hand, the triple-band Hartley VCO has achieved a low-band oscillation of 0.98 GHz, a middle-band oscillation of 1.04 GHz, and a high-band oscillation of 1.22 GHz. The measured and simulated oscillation frequencies are in good agreement for three different conditions. Measured SSB (Single Side Band) noise of the triple-band Clapp oscillator were shown in Fig. 7. The phase noise at 100 kHz offset varies

from -93 to -102 dBc/Hz. Measured SSB (Single Side Band) noise of the triple-band Hartley oscillator were shown in Fig. 8. The phase noise at 100 kHz offset varies from -84 to -94 dBc/Hz.

## 6 Conclusions

Design, simulation, fabrication and, a performance of the triple-band SiGe HBT Clapp and Hartley oscillators using the stacked element-selective transistors have been demonstrated. It has been clearly shown that a triple-band oscillator becomes available by switching only two circuit elements with the use of the stacked element-selective transistors. The stacked element-switching technique introduced in this paper would be one candidate for miniaturization of the multi-band oscillations for use in the next generation multi-band and / or multi-mode wireless radios.

## References

- [1] A.A. Abidi, RF CMOS Comes of Age, *IEEE Microwave Magazine*, **4**, no. 4, (2003), 47-60. <https://doi.org/10.1109/mmw.2003.1266066>
- [2] N. Buadana and E. Socher, A Triple Band Travelling Wave VCO Using Digitally Controlled Artificial Dielectric Transmission Lines, *2011 IEEE Radio Frequency Integrated Circuits Symposium*, 2011, 1-4. <https://doi.org/10.1109/rfic.2011.5940705>
- [3] W. Cao, Y. Tashiro, and Y. Itoh, A Dual-Band SiGe HBT Differential VCO Using a Control Voltage for both Band-Switching and Frequency-Tuning, *Proceeding of the Asia-Pacific Microwave Conference*, December 2010, 449-452.
- [4] Y. Itoh, H. Hasegawa, M. Shirata, and K. Sakamoto, Supply Voltage Switching Dual-Band SiGe HBT VCOs Using a Dual-Band Resonator with Inductor-Loaded Varactor Diodes, *IEEE IMS Digest*, 2009, 1289-1292. <https://doi.org/10.1109/mwsym.2009.5165940>
- [5] Y. Itoh and S. Tanaka, A Triple-Band SiGe HBT Differential VCO Using a Reconfigurable Multi-Band Resonator, *Proceeding of the 40th European Microwave Conference*, September 2010, 456-459.
- [6] Y. Itoh, W. Xiaole and S. Omokawa, A Triple-Band SiGe HBT Cross-Coupled Differential VCO Using a Novel Element-Switching Technique, *Proceedings of the 2018 Asia Pacific Microwave Conference, WE1-1F-1*, November 2018. <https://doi.org/10.23919/apmc.2018.8617512>



- [7] S. Jain and S.L. Jang, Triple-Band Transformer-Coupled LC Oscillator with Large Output Voltage Swing, *IEEE Microwave and Wireless Components Letters*, **24**, No. 7 (2014), 475-477.  
<https://doi.org/10.1109/lmwc.2014.2316493>
- [8] A.R. Rofougaran, M. Rofougaran and A. Behzad, Radios for Next-Generation Wireless Networks, *IEEE Microwave Magazine*, **6**, no. 1 (2005), 38-43. <https://doi.org/10.1109/mmw.2005.1417993>
- [9] U.L. Rohde and A.K. Poddar, Multi-mode multi-band tunable active inductor oscillators, *2011 Joint Conference of the IEEE International Frequency Control and the European Frequency and Time Forum (FCS) Proceedings*, 2011. <https://doi.org/10.1109/fcs.2011.5977283>
- [10] H. Wang, F. Zhao, F.F. Dai, G. Niu, B. Wilamowski, J. Fu, W. Zhou and Y. Wang, A Wide Tuning Triple-Band Frequency Generator MMIC in 0.18 $\mu\text{m}$  SiGe BiCMOS Technology, *2014 IEEE Bipolar/BiCMOS Circuits and Technology Meeting (BCTM)*, 2014.  
<https://doi.org/10.1109/bctm.2014.6981314>

**Received: October 12, 2019; Published: November 15, 2019**